ChemComm

COMMUNICATION

View Article Online
View Journal | View Issue



Check for updates

Cite this: *Chem. Commun.*, 2025, **61**, 19493

Received 24th August 2025,
Accepted 10th November 2025

DOI: 10.1039/d5cc04816h

rsc.li/chemcomm

# Controlling Lewis acid-catalysed bicyclobutane cycloadditions: carbonyl substituents dictate electrophilic *vs.* nucleophilic addition pathways

Dan Liu,[a] Ning Wang,[bc] Yuhong Yang,[bc] Qing Zou[b] and Xiaoyong Zhang *[b]

**Combined DFT and DLPNO-CCSD(T) mechanistic studies reveal that carbonyl substituents of bicyclobutane (BCB) dictate the reaction pathways in Lewis acid-catalysed BCB-imine cycloadditions, toggling between electrophilic and nucleophilic additions, as well as concerted and stepwise ring-opening/addition mechanisms.**

Driven by the "escape from flatland" concept in medicinal chemistry, three-dimensional bridged cyclic hydrocarbons have received growing interest in recent years.[1] These strained architectures, including bicyclo[2.1.1]hexanes (BCHs) and bicyclo[3.1.1]heptanes (BCHeps), offer superior properties such as improved solubility and better metabolic stability compared to traditional aromatic frameworks. In particular, BCHs have emerged as valuable bioisosteres capable of mimicking *ortho*- and *meta*-substituted benzenes while providing distinct three-dimensionality.

The synthesis of BCHs has been significantly advanced through cycloaddition chemistry of bicyclo[1.1.0]butanes(BCBs) *via* thermo-driven,[2] Lewis-acid catalysed,[3,4] photocatalysed,[5] or radical-based[6] catalysed reactions. Among them, Lewis acid catalysis has proven to be a versatile and efficient strategy to access BCHs from BCBs.[7] Continuous contributions from groups including Leitch, Studer, Glorius, Deng, Feng, Biju, Bach, Shi, Zhou, Li, and Han have significantly advanced this field,[3,4] enabling cycloaddition of BCBs with a diverse range of unsaturated substrates. Notably, recent advances now enable asymmetric synthesis of enantioenriched BCH.[8] Despite significant advances in the synthetic applications of Lewis acid-catalysed BCB cycloadditions, the underlying reaction mechanisms remain poorly understood.[3,4,9]

Competing hypotheses (Scheme 1) suggest that Lewis acid coordination may either: (1) enhance the electrophilic character of the BCB moiety, facilitating addition with various nucleophiles including indoles and ynamides (nucleophilic addition pathway),[3] or (2) activate the BCB as a nucleophile to react with electron-deficient partners (electrophilic addition pathway).[4] The latter pathway requires particular attention as the cycloaddition competes with potential E1 elimination.[4a,4b] Notably, many[3l–o,4a–h] of these studies have proposed that Lewis acid activation might induce direct cleavage of the bridge C–C bond in BCB, generating a zwitterionic enolate intermediate that subsequently attacks unsaturated substrates through a stepwise mechanism rather than a concerted ring-opening/addition pathway. Given these mechanistic complexities, our ability to selectively steer these competing pathways remains limited.

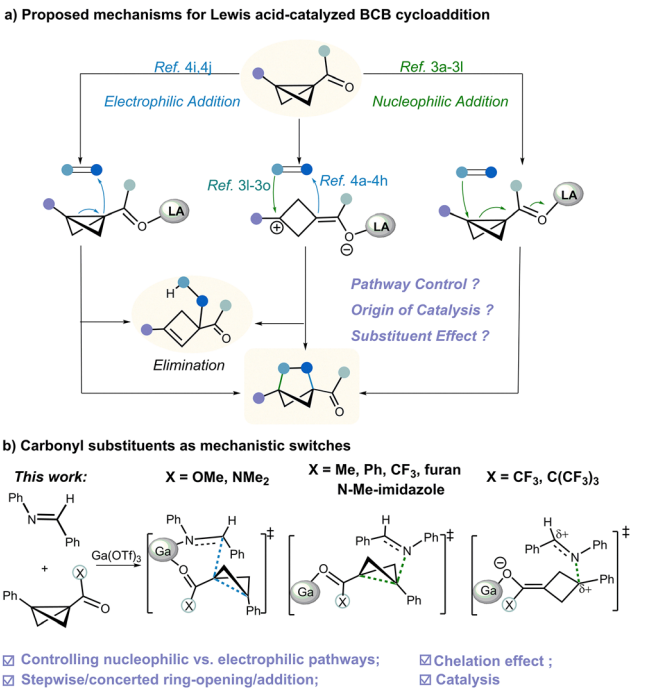


Scheme 1 Mechanistic considerations of Lewis-acid catalysed cycloaddition of BCB.

[a] *School of Science, Changchun Institute of Technology, Changchun 130012, China*
[b] *Guangdong Provincial Key Laboratory of Mathematical and Neural Dynamical Systems, School of Sciences, Great Bay University, Dongguan, 523000, China. E-mail: zhangxiaoyong@gbu.edu.cn*
[c] *Department of Chemistry, Southern University of Science and Technology, Shenzhen, China*

Current experimental approaches to controlling BCB cycloaddition pathways primarily focus on modulating the electronic properties of the unsaturated coupling partners.[3a–d] However, our recent studies indicated that the electronic characteristics of BCB active species play a key role in pathway selection.[10] Building upon this insight, we now computationally demonstrate that modifying the BCB carbonyl substituents (X = OMe, $NMe_2$, Me, Ph, $CF_3$, $C(CF_3)_3$, N-Me-imidazole and furan) is a feasible strategy to control reaction pathways using the same coupling partner.

Our mechanistic investigation begins with the $Ga(OTf)_3$-catalysed cycloaddition of BCB ester **2a** with *N*-aryl imine **1a**, given the rich experimental data. Calculations using the DLPNO-CCSD(T)/def2-TZVP(SMD)//SMD(THF) B3LYP-D3/6-31G(d) method confirm the electrophilic addition pathway,[4a] but initiates with favorable bi-coordination of both substrates to Ga, forming stable intermediate $\mathbf{IN1_{2a}}$ (Fig. 1a), However, contrary to prior proposals, the ring-opening and addition proceeds concertedly *via* $\mathbf{TS1E_{2a}}$ ($\Delta G^{\ddagger}$ = 16.4 kcal $mol^{-1}$) to give $\mathbf{IN2_{2a}}$, not through a stepwise process. The alternative nucleophilic addition pathway proves energetically less favorable ($\mathbf{TS1N_{2a}}$, $\Delta G^{\ddagger}$ = 24.3 kcal $mol^{-1}$) due to the requirement of imine dissociation from Ga(III) to attack the distal BCB carbon atom.[11] This dissociation is thermodynamically unfavourable, as evidenced by the complex formed by **Ga**/**2a** and the uncoordinated imine lying 9.7 kcal $mol^{-1}$ higher in energy than $\mathbf{IN1_{2a}}$.

While the major product for **2a** is the cycloadduct, intermediate $\mathbf{IN3_{2a}}$ can undergo competitive E1 elimination (Fig. S2). For **2a**, the elimination product is thermodynamically disfavored by 3.0 kcal $mol^{-1}$ relative to the cycloaddition product. Nevertheless, *tert*-butyl substitution on the imine stabilizes the E1 product by 7.8 kcal $mol^{-1}$ lower than the cycloaddition product, and drives the reaction exclusively toward E1 elimination. These calculations are in perfect agreement with experimental observations, which provides robust validation of our calculation model.

Remarkably, introducing a methyl substituent at the BCB carbonyl group induces a complete mechanistic inversion, shifting the dominant pathway from electrophilic to nucleophilic addition (Fig. 1b). This nucleophilic pathway proceeds through a concerted ring-opening/nucleophilic addition TS ($\mathbf{TS1N_{2b}}$, $\Delta G^{\ddagger}$ = 17.7 kcal $mol^{-1}$), which serves as the rate-determining step. Nevertheless, the competing electrophilic pathway ($\mathbf{TS1E_{2b}}$) becomes disfavored by 3.9 kcal $mol^{-1}$. Compared to BCB ester, this ketone derivative clearly exhibits significantly enhanced reactivity toward nucleophilic attack—despite similarly unfavorable imine dissociation—highlighting the critical role of substituent effects in driving the observed mechanistic switch. Further evaluations of $NMe_2$- and Ph-substituted BCBs suggest the electronic control of pathway selectivity. The Ph-system displays comparable pathway selectivity and activation barriers to the Me-system, whereas the amide analogue with strong electron-donating character follows the behavior observed for BCB ester (Fig. S4 and S5).

Our distortion/interaction-activation strain (D/IAS) analysis reveals that while the Ga-coordinated **2b**/imine system exhibits faster-growing distortion energy along the nucleophilic addition reaction coordinate compared to the BCB ester analogue (Fig. 2), this penalty is more than compensated by significantly stronger inter-fragment interactions, making nucleophilic addition the dominant pathway for BCB ketone. Further energy decomposition analysis (EDA)[12] pinpoints the enhanced interactions arising from superior electrostatic interactions, and pronounced induction (including polarization and charge transfer) between the Ga-activated **2b** and imine components. Frontier molecular orbital (FMO) analysis suggests that the interaction energy differences mainly originate from fundamental electronic restructuring. The LUMO of the Lewis acid-activated BCB ketone is substantially

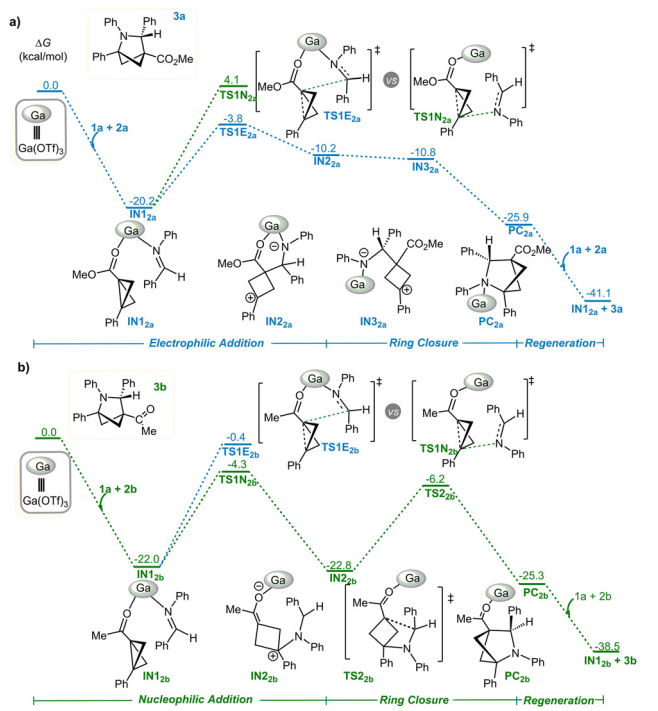


Fig. 1 Free energy profile (in kcal $mol^{-1}$) of Lewis acid-catalysed cycloaddition of BCB substrate. (a) X = OMe; (b) X = Me.

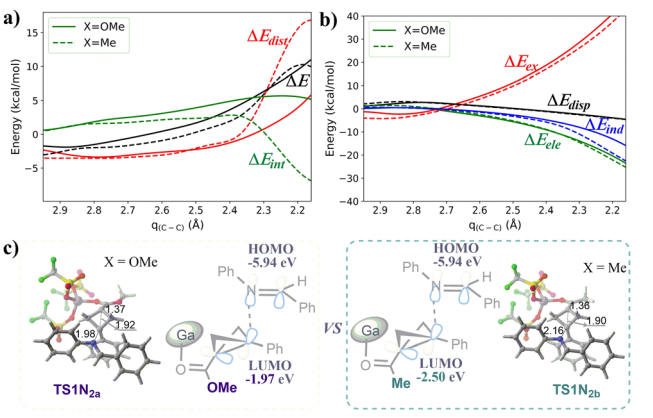


Fig. 2 Energy decomposition analysis for BCB ketone and ester reactivity. (a) Comparison of distortion and interaction energies. (b) Breakdown of interaction energy components. (c) Frontier orbital interaction and transition state geometries with key bond lengths (Å).

stabilized (−2.50 eV) relative to the ester analogue (−1.97 eV), reflecting the weaker electron-donating ability of Me than OMe. This stabilization narrows the HOMO(imine)–LUMO(Ga-BCB) gap from 3.97 (OMe) to 3.44 eV (Me). This orbital energy modulation directly correlates with the lower nucleophilic addition barrier for BCB ketones (17.7 kcal $mol^{-1}$) compared to esters (24.3 kcal $mol^{-1}$). Collectively, these findings establish a clear structure-mechanism relationship: subtle modifications at the BCB carbonyl group (ester → ketone) can profoundly redirect the reaction pathways by tuning frontier orbital energies and intermolecular interaction patterns.

Comparative analysis of OMe- and Me-substituted BCBs reveals another intriguing finding concerning the viability of the proposed stepwise ring-opening/addition pathway.[3l–o,4a–h] For **2a** and **2b**, the putative Ga-bound ring-opened enolate intermediates and associated transition states are energetically disfavoured relative to the concerted pathway, ruling out the stepwise mechanism (Fig. 3 and Fig. S6). Nevertheless, we observe a progressive increase in thermodynamic stability of the intermediate across the series (OMe → Me), suggesting a potential carbonyl substituent-driven "stepwise-concerted" pathway shift by modifying the electron donating or withdrawing ability. Calculations using the $CF_3$-substituted BCB show that the energy barrier difference between the two pathways is rather small (∼1.1 kcal $mol^{-1}$), rendering them degenerate, while $C(CF_3)_3$ completely suppresses the concerted path, enabling only the stepwise mechanism. These findings establish that carbonyl substituents can also serve as powerful mechanistic switches between concerted and stepwise pathways.

Next, we studied BCB functionalized with an *N*-methylimidazole group (**2c**)-transforming it into a privileged bidentate substrate that is widely utilized in cycloaddition reactions.[3j] The reaction profile of **2c** exhibits unique mechanistic features (Fig. S7), favouring a nucleophilic addition pathway analogous to BCB ketones but distinguished by its metal coordination behaviour (Fig. 4). The bidentate coordination mode (*via* BCB carbonyl oxygen and imidazole nitrogen) of substrate **2c** generates an exceptionally stable intermediate (**IN1$_{2c}$**, −42.1 kcal $mol^{-1}$), in which imine is also coordinated to Ga. Nucleophilic addition

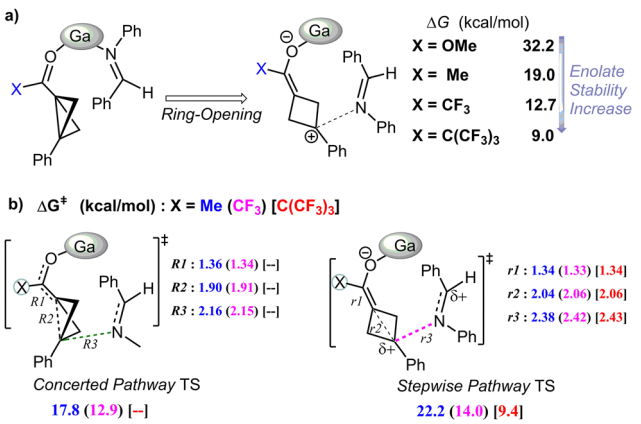


Fig. 3 (a) Thermodynamics of direct ring opening of BCB; (b) overall barrier of the nucleophilic addition transition state.

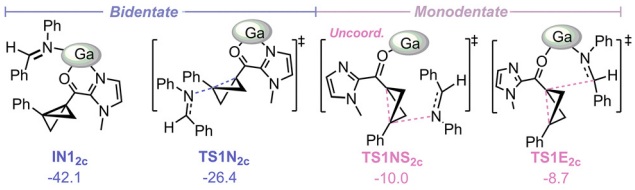


Fig. 4 Free energy (kcal $mol^{-1}$) of key species in Lewis acid-catalysed cycloaddition of BCB substrate **2c** with chelating substituent N-Me-imidazole.

proceeds *via* a dissociative transition state (**TS1N$_{2c}$**, $\Delta G^{\ddagger}$ = 15.7 kcal $mol^{-1}$) where the imine dissociates to attack the BCB. The bidentate chelation is critical, as it drastically stabilizes the pathway, with the monodentate coordination exhibiting a 16.4 kcal $mol^{-1}$ higher barrier. This stabilization as well creates a 17.7 kcal $mol^{-1}$ energy gap between nucleophilic and electrophilic pathways, effectively suppressing the latter. Comparably, a weaker-coordinating furan substituent forms a less stable complex (−26.3 kcal $mol^{-1}$) and narrows the pathway gap to just 2.6 kcal $mol^{-1}$ (Fig. S8), confirming that strong chelators preferentially stabilize nucleophilic addition transition states.

Finally, we elucidate the catalytic origin of Lewis acid catalysis in the nucleophilic addition pathway. In the absence of $Ga(OTf)_3$, the nucleophilic addition TSs of **2b**/**2c** are energetically disfavoured by 23.8–27.3 kcal $mol^{-1}$. Our D/IAS calculations demonstrate that the driving force of catalysis originates from the significantly enhanced intermolecular interactions between activated BCB and imine (Fig. 5a). EDA identifies the stabilization mechanism as a combination of reduced exchange repulsion and enhanced induction interactions for **2b** and **2c** (Fig. 5b and Fig. S9). Orbital analysis further rationalizes these effects: Ga(III) coordination lowers both the HOMO and LUMO energies of the BCB substrate. This dual orbital tuning creates an optimal electronic environment by: (i) minimizing HOMO–HOMO repulsion between reactants (consistent with the Pauli repulsion-lowering catalysis strategy proposed by Hamlin *et al.*[13]), which accounts for ∼60% of the total catalytic stabilization, and (ii) enhancing HOMO(imine)–LUMO(BCB) overlap, facilitating efficient electron transfer (Fig. 5c). Thus, the catalytic role of Ga in the nucleophilic addition pathway arises from the synergistic effects of Pauli repulsion-lowering and LUMO-lowering action. Notably, while the LUMO orbital shows significant distribution on the carbonyl carbon site, calculations confirm that nucleophilic attack at this position is kinetically disfavoured, with an energy barrier consistently >6.0 kcal $mol^{-1}$ higher than that at the bridgehead carbon across all BCB derivatives (Fig. S10).

In summary, this communication demonstrates how carbonyl substituents of BCB dictate reaction pathways in Lewis acid-catalysed BCB-imine cycloadditions, establishing a framework for controlling strained ring reactivity through rational substituent design.

We thank the National Natural Science Foundation of China (12504333), and Guangdong Basic and Applied Basic Research Foundation (2022A1515110835 and 2025A1515010088) for funding this work. The computational resources are supported by SongShan Lake HPC Center (SSL-HPC) in Great Bay University.

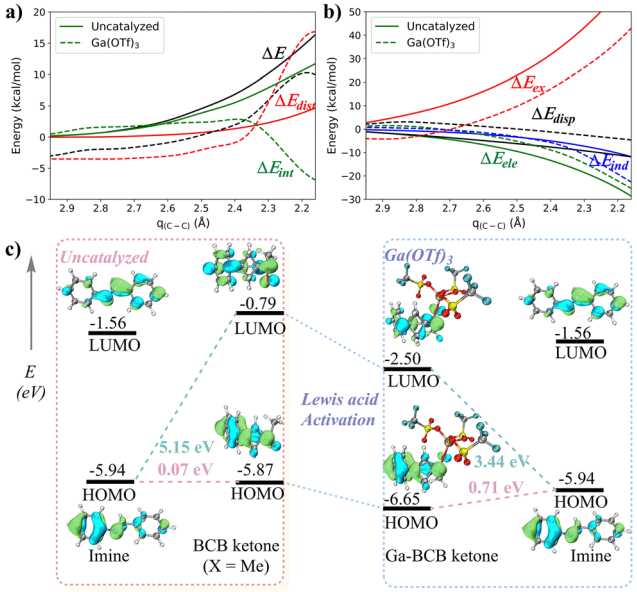


Fig. 5 (a) D/IAS and (b) EDA along the reaction coordinate of nucleophilic addition for uncatalysed and catalysed cycloadditions of BCB ketone, and (c) frontier orbital interaction diagram.

## Conflicts of interest

There are no conflicts to declare.

## Data availability

The data supporting this article have been included as part of the supplementary information (SI). Supplementary information: computational details, free energy profiles of varying BCB derivatives, absolute energies and coordinates. See DOI: **https://doi.org/10.1039/d5cc04816h**.

## Notes and references

1 (*a*) C. B. Kelly, J. A. Milligan, L. J. Tilley and T. M. Sodano, *Chem. Sci.*, 2022, **13**, 11721; (*b*) J. Tsien, C. Hu, C. R. R. Merchant and T. Qin, *Nat. Rev. Chem.*, 2024, **8**, 605.

2 T. Hoshikawa, K. Tanji, J. Matsuo and H. Ishibashi, *Chem. Pharm. Bull.*, 2012, **60**, 548.

3 BCB cycloaddition proposed with the nucleophilic addition pathway: (*a*) Q. Q. Hu, L. Y. Wang, X. H. Chen, Z. X. Geng, J. Chen and L. Zhou, *Angew. Chem., Int. Ed.*, 2024, **63**, e202405781; (*b*) S. Hu, Y. M. Pan, D. S. Ni and L. Deng, *Nat. Commun.*, 2024, **15**, 6128; (*c*) D. Ni, S. Hu, X. Tan, Y. Yu, Z. Li and L. Deng, *Angew. Chem., Int. Ed.*, 2023, **62**, e202308606; (*d*) D. Sarkar, S. Deswal, R. C. Das and A. T. Biju, *Chem. Sci.*, 2024, **15**, 16243; (*e*) K. J. Woelk, K. Dhake, N. D. Schley and D. C. Leitch, *Chem. Commun.*, 2023, **59**, 13847; (*f*) L. Tang, K. J. Wang, L. Wang, F. J. Yang, Q. X. Peng, G. Q. Wang and J. J. Feng, *Sci. China: Chem.*, 2025, DOI: **10.1007/s11426-025-2698-2**; (*g*) J. Yang, B. X. Yao, H. F. Jiang, S. F. Ni, P. H. Dixneuf and M. Zhang, *Angew. Chem., Int. Ed.*, 2025, **64**, e202505060; (*h*) S. J. Zhu, X. Tian and S. W. Li, *Org. Lett.*, 2024, **26**, 6309; (*i*) L. Tang, W. J. Bai, K. J. Wang, F. Wu, Q. X. Peng, G. P. Huang and J. J. Feng, *ACS Catal.*, 2025, **15**, 7877; (*j*) F. Wu, W. B. Wu, Y. J. Xiao, Z. X. Li, L. Tang, H. X. He, X. C. Yang, J. J. Wang, Y. L. Cai, T. T. Xu, J. H. Tao, G. Q. Wang and J. J. Feng, *Angew. Chem., Int. Ed.*, 2024, **63**, e202406548; (*k*) R. Meher and S. C. Pan, *Org. Chem. Front.*, 2025, **12**, 5908; (*l*) X.-G. Zhang, J.-J. Chen, Z.-Y. Zhou, J.-X. Li and Q.-L. Zhou, *Chem. Catal.*, 2025, **5**, 101295; (*m*) H. S. Ren, Z. R. Lin, T. X. Li, Z. Y. Li, X. H. Yu and J. Zheng, *ACS Catal.*, 2025, **15**, 4634; (*n*) J. L. Li, C. Xie, R. Zeng, W. C. Yuan, Y. Y. Lei, T. Qi, H. J. Leng and Q. Z. Li, *ACS Catal.*, 2025, **15**, 6025; (*o*) Y. Liang, R. Nematswerani, C. G. Daniliuc and F. Glorius, *Chem. Commun.*, 2025, **61**, 2091.

4 BCB cycloaddition proposed with the electrophilic addition pathway: (*a*) K. Dhake, K. J. Woelk, J. Becica, A. Un, S. E. Jenny and D. C. Leitch, *Angew. Chem., Int. Ed.*, 2022, **61**, e202204719; (*b*) Y. J. Liang, F. Paulus, C. G. Daniliuc and F. Glorius, *Angew. Chem., Int. Ed.*, 2023, **62**, e202305043; (*c*) K. Hu, H. Wu, M. Sun, J. Zhang, Z. Wang, J. Yang, G. Zhu and G. B. Huang, *Chem. Commun.*, 2025, **61**, 10375; (*d*) Q. Jiang, J. Y. Dong, D. J. Yu, F. Lei, T. Li, T. F. Kang, J. Fan, H. M. Sun and D. Xue, *Org. Chem. Front.*, 2025, **12**, 5293; (*e*) J.-Y. Su, J. Zhang, Z. Y. Xin, H. Li, H. Zheng and W. P. Deng, *Org. Chem. Front.*, 2024, **11**, 4539; (*f*) H. J. Wu, M. M. Sun, J. Zhang, Z. M. Wang, J. G. Yang and G. G. Zhu, *Org. Chem. Front.*, 2025, **12**, 1951; (*g*) K. Zhang, S. H. Tian, W. K. Li, X. Yang, X. H. Duan, L. N. Guo and P. F. Li, *Org. Lett.*, 2024, **26**, 5482–5487; (*h*) L. Xiao, L. Li, Y. S. Xiong, Y. F. Zhao, D. W. Stephan and J. Guo, *Org. Lett.*, 2025, **27**, 7302; (*i*) R. Lu, J. Yang, J. M. Jiang, J. Wang, W. Huang, C. Peng, G. Zhan and B. Han, *JACS Au*, 2025, **5**, 2738; (*j*) J. Jeong, S. Cao, H. J. Kang, H. Yoon, J. Lee, S. Shin, D. Kim and S. Hong, *J. Am. Chem. Soc.*, 2024, **146**, 27830.

5 (*a*) Y. C. Chang, M. Martín, K. Bortey, Q. Lefebvre, T. Fessard, C. Salome, R. J. Vázquez and M. K. Brown, *J. Am. Chem. Soc.*, 2025, **147**, 14936; (*b*) R. Kleinmans, T. Pinkert, S. Dutta, T. O. Paulisch, H. Keum, C. G. Daniliuc and F. Glorius, *Nature*, 2022, **605**, 477; (*c*) Y. J. Liang, R. Kleinmans, C. G. Daniliuc and F. Glorius, *J. Am. Chem. Soc.*, 2022, **144**, 20207.

6 (*a*) S. Agasti, F. Beltran, E. Pye, N. Kaltsoyannis, G. E. M. Crisenza and D. J. Procter, *Nat. Chem.*, 2023, **15**, 535; (*b*) T. Yu, X. Zhao, Z. C. Nie, L. L. Qin, Z. W. Ding, L. Xu and P. F. Li, *Angew. Chem., Int. Ed.*, 2025, **64**, e202420831.

7 (*a*) X. Liu, J. W. He, K. Y. Lin, X. Y. Wang and H. Cao, *Org. Chem. Front.*, 2024, **11**, 6942; (*b*) S. J. Sujansky and X. S. Ma, *Asian J. Org. Chem.*, 2024, **13**, e202400045; (*c*) H. Yang, J. Chen and L. Zhou, *Synlett*, 2025, 788.

8 (*a*) Y. Koo, J. Jeong and S. Hong, *ACS Catal.*, 2025, **15**, 8078; (*b*) X. C. Yang, J. J. Wang, Y. J. Xiao and J. J. Feng, *Angew. Chem., Int. Ed.*, 2025, **64**, e202505803; (*c*) L. Alama, N. Frank, L. Brücher, J. Nienhaus and B. List, *ACS Catal.*, 2025, **15**, 8297; (*d*) J. T. Che, W. Y. Ding, H. B. Zhang, Y. B. Wang, S. H. Xiang and B. Tan, *Nat. Chem.*, 2025, **17**, 393.

9 (*a*) J. J. Wang, L. Tang, Y. J. Xiao, W. B. Wu, G. Q. Wang and J. J. Feng, *Angew. Chem., Int. Ed.*, 2024, **63**, e202405222; (*b*) F. H. Zhang, S. Dutta, A. Petti, D. Rana, C. G. Daniliuc and F. Glorius, *Angew. Chem., Int. Ed.*, 2025, **64**, e202418239.

10 (*a*) D. Liu, X. F. Guo, S. Y. Zhou, L. X. Guo and X. Y. Zhang, *J. Org. Chem.*, 2024, **89**, 1241; (*b*) N. Radhoff, C. G. Daniliuc and A. Studer, *Angew. Chem., Int. Ed.*, 2023, **62**, e202304771.

11 The intermolecular nucleophilic attack of a second imine to $IN1_{2a/2b}$ is energetically comparable to $TS1N_{2a/2b}$ (see Fig. S3).

12 (*a*) A. Sengupta, B. Li, D. Svatunek, F. Liu and K. N. Houk, *Acc. Chem. Res.*, 2022, **55**, 2467; (*b*) K. Szalewicz, *WIREs Comput. Mol. Sci.*, 2012, **2**, 254.

13 T. A. Hamlin, F. M. Bickelhaupt and I. Fernández, *Acc. Chem. Res.*, 2021, **54**, 1972.